Project 059(D) Physics-Based Analyses and Modeling for Supersonic Aircraft Exhaust Noise

Stanford University

Project Lead Investigator

Sanjiva K. Lele
Professor
Department of Aeronautics & Astronautics
Stanford University
Durand Building
496 Lomita Mall
Stanford, CA 94305
650-723-7721
lele@stanford.edu

University Participants

Stanford University

- P.I.s: Dr. Sanjiva K. Lele and Dr. Juan J. Alonso
- FAA Award Number: 13-C-AJFE-SU-024
- Period of Performance: January 1, 2022 to December 16, 2022
- Tasks:
    1. Develop and refine research plans in coordination with ASCENT Project 59 partners
    2. Large eddy simulation (LES)-based simulation, modeling, and validation of jet noise predictions
    3. Reynolds-averaged Navier–Stokes (RANS)-based simulation, modeling, and validation of jet noise predictions

Project Funding Level

This project received $200,000 per year from the FAA; in-kind matching from Stanford; and cost-share matching from Gulfstream.

Investigation Team

Dr. Sanjiva K. Lele (P.I.), Department of Aeronautics and Astronautics, Stanford University
Dr. Juan J. Alonso (P.I.), Department of Aeronautics and Astronautics, Stanford University
Gao Jun Wu, PhD student, Department of Aeronautics and Astronautics, Stanford University
Tejal Shanbhag, PhD student, Department of Aeronautics and Astronautics, Stanford University
Kristen Matsuno, PhD student, Department of Mechanical Engineering, Stanford University
Olivia Martin, PhD student, Department of Mechanical Engineering, Stanford University

Project Overview

Improved methods for prediction and reduction of noise for civil supersonic aircraft would be highly valued by the research and technology development community engaged in civil supersonic aircraft development. Beyond the aircraft and engine companies, organizations such as NASA, the FAA, and the Department of Defense research and technology community would also benefit from the improved methods and tools. Ultimately, supersonic jet noise tools with predictive capabilities can be used to design better noise mitigation systems and to provide estimates of noise for certification studies.

The project involves coordinated development of both low- and high-fidelity approaches for jet noise predictions for civil supersonic aircraft being considered in ASCENT, including the tasks listed above. High-fidelity simulations of the jet exhaust

flow and noise will be developed for a carefully selected subset of configurations and operating points being tested by the Georgia Institute of Technology (Georgia Tech) team. In parallel, RANS computations of a broader range of configurations and operating conditions relevant to civil supersonic aircraft will be performed and used to develop improved jet noise source models and more accurate far-field noise propagation kernels. The noise source and noise propagation modeling will leverage high-fidelity simulation data and ongoing Georgia Tech experiments, as well as other noise and flow measurements available in the archival literature. Our goal is to understand the predictive quality of RANS-based noise prediction approaches with improved source and/or propagation models, to enable designers to better capture the trade-offs typical in the development of full civil supersonic aircraft configurations.

Task 1 - Develop and Refine Research Plans in Coordination with ASCENT Project 59 Partners

Stanford University

Objectives

We aim to determine a plan for the simulation study that covers the range of operating conditions and possible nozzle configurations relevant to civil supersonic jet exhaust. The plan must include the current test plan from our experimental partner at Georgia Tech.

Research Approach

The planning involved discussions with Project 59 partners and reaching out to external advisors at NASA and elsewhere in academia and industry. On the basis of this exercise, a decision was made that the project should focus on axisymmetric dual-stream nozzles with an internal mixer, and the possibility of an internal and/or external nozzle plug. We also searched for nozzle configurations, and flow and noise measurement data in archival literature, which would be deemed relevant for civil supersonic aircraft and could be used in the development of noise prediction methods. Comprehensive exploration indicated that the bulk of jet noise data including studies of noise reduction concepts was in the regime of moderate-to-high BPR and thus not particularly relevant to civil supersonic aircraft. Although these findings affirmed the need for the planned laboratory measurement campaign by Project 59 partner Georgia Tech, they also highlighted the need to use the most relevant data from the published literature to kickstart the modeling and simulation efforts. Two specific data sets associated with jet noise tests at NASA Glenn Research Center were thus identified.

Georgia Tech Dual Stream Nozzle

A co-annular nozzle geometry with a variable-length mixing duct is designed and being tested extensively by the team at Georgia Tech. After discussions among the project collaborators and key stakeholders, a test matrix has been determined for the Year 1 and 2 experimental efforts. The jet Mach number for each of the two streams varies between $M_j = 0.4$ and $M_j = 1.0$, and the length of the nozzle mixing duct can be adjusted to be 0.7, 1.0, 2.0, or 3.0 times the length of the nozzle diameter, $D_e = 1.7$ inches.

Bridges and Wernet Internal Mixer

In 2004, Bridges and Wernet (NASA Glenn Research Center) reported flow and noise measurements for internally mixed two-stream nozzles with variations in the mixer duct length and mixer geometry. The operating conditions involve transonic and low-supersonic jet exhaust velocity and moderate BPR. This configuration has been used in previous RANS-based noise prediction studies by Rolls Royce and Purdue University, along with a more recent LES study. We have been in touch with Rolls Royce and NASA regarding the nozzle geometry and the measurement data. We hope that the geometry and data will become available to us in the future. This configuration is of interest to us, because it is unique in providing both jet flow measurements and far-field noise at conditions relevant to civil supersonic flights.

Recent Jet Noise Measurements at NASA Glenn Research Center

As part of NASA's Commercial Supersonic Technology Project, under the Advanced Aero Vehicle Program, Dr. James Bridges at NASA Glenn Research Center (personal communication, 2020) recently completed jet noise measurements on specially designed modular nozzle configurations at operating points selected to be relevant to commercial supersonic aircraft. He plans to make the nozzle geometry and measurement data available in the future. NASA's plans include noise predictions using a variety of computational tools. We are interested in exploring a selected subset of NASA's test matrix in our Project 59 studies. We have obtained the computer-aided-design geometry for the nozzle and have begun early efforts in geometry

cleaning and mesh generation. The mesh generation for this case is fairly challenging, because of the steep curvature and sharp edges in the mixer lobes.

Milestones
The simulation plan for Years 1–2 has been determined and followed. Our plan for Year 3, regarding nozzles with noise mitigation concepts, is being finalized, with a focus on studying the effects of mixing enhancement devices at heated jet conditions.

Major Accomplishments
A research plan regarding the nozzle geometry and flow conditions to be studied has been developed. The plan includes both the experimental study by our partner at Georgia Tech and other relevant work from NASA Glenn Research Center.

Publications
None.

Outreach Efforts
Communication with researchers at NASA Glenn Research Center has been established, and ideas for possible collaboration have been exchanged.

Awards
None.

Student Involvement
Three graduate students are involved in this part of the project. G. Wu and K. Matsuno have conducted literature research on relevant jet experiments and simulations involving similar flow conditions and nozzle mixing devices. T. Shanbhag has conducted literature reviews on acoustic modeling of jet noise. K. Matsuno completed her PhD recently. O. Martin has joined the project and is helping with the simulations of the mixer nozzle.

Plans for Next Period
We will continue to refine our research plan according to the ongoing discussions among teams of Project 59. In particular, we will select nozzle geometries with noise mitigation concepts of interest to the industrial partners for the development of next-generation supersonic civil transport aircraft.

Task 2 - LES-based Simulation, Modeling, and Validation of Jet Noise Predictions
Stanford University

Objectives
In collaboration with ASCENT partners in Project 59, we plan to develop physics-based analyses for supersonic aircraft exhaust noise. The main goals of these analyses are to develop improved jet noise prediction methods by using a multi-fidelity approach. As part of the high-fidelity approach, LES will be conducted for a carefully selected set of configurations and operating points corresponding to tests conducted by the experimental team at Georgia Tech. The LES data will provide the turbulence flow statistics and will be leveraged for acoustic source modeling.

Research Approach
In the past project year, the high-fidelity modeling efforts have focused on the dual-stream conical nozzle designed and tested by Georgia Tech. The nozzle exit diameter, D_e, is 1.7 inches, and a mixing duct with adjustable length with respect to the nozzle diameter is present. LES and far-field acoustics modeled by the permeable Ffowcs Williams and Hawkings (FW-H) formulation are obtained by using the compressible solver CharLES, developed by Cascade Technologies. Work in Year 1 has been published in a conference manuscript (Wu et al., 2022). In the manuscript, we report results at $M_j = 0.8, 0.9$ for the geometry with the shortest mixing duct, $L/D_e = 0.7$. However, the comparison of noise spectra between LES and available

measurements showed spurious numerical artifacts at high frequencies. During project Year 2, we have focused on determining the causes of such discrepancies with a mesh sensitivity study. With improved mesh resolution in the jet shear layers, errors at the high-frequency range have been reduced. Further validation of LES results has been performed with more recent experimental measurements from Georgia Tech. Turbulence statistics from the improved LES data sets are then used to support the development of RANS-based acoustic source models, as discussed in Task 3.

Progress in Jet Noise Modeling and Simulations

The nozzle geometry was designed and tested by the Project 59 partner at Georgia Tech (Figure 1). The area ratio of the secondary to the primary nozzle is 2.25. An exhaust mixing duct is attached to the end of the co-annular nozzle, and the length of the mixing duct is 0.7 D_e. LES of the jet exhaust flow and noise is conducted at $M_j = 0.8$ for both the primary conical nozzle alone and the co-annular nozzle. For the primary nozzle test case, iterative mesh refinement is performed among four different meshes. For the co-annular nozzle, a moderate mesh design is selected on the basis of the analysis of the primary nozzle test case. Table 1 provides a summary of all test cases.

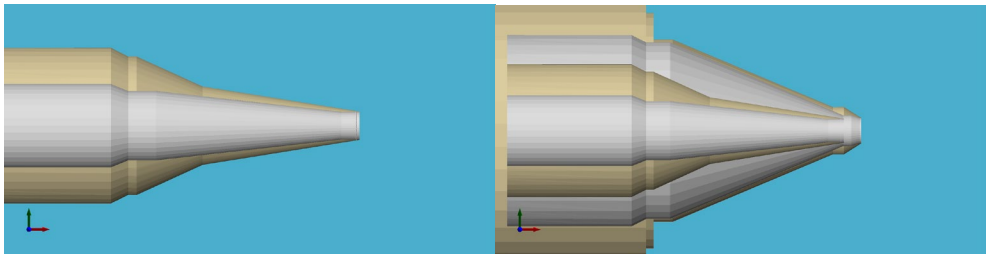

Figure 1. Left: primary nozzle. Right: co-annular nozzle designed by Georgia Tech.

Table 1. Summary of the test cases. All flow conditions are non-heated.

M_{j1}	M_{j2}	Mesh cell count in millions (mesh label)	LES simulation time $t_{sim}\, c_\infty/D_{e1}$
0.8	N/A	18 (A), 27 (B), 98 (C), 131 (D)	700
0.8	0.8	30 (coB)	900

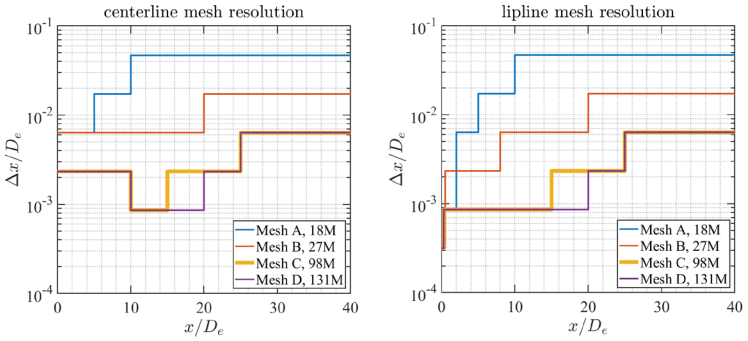

Figure 2. Mesh resolutions along the centerline (left) and the lipline (right) for the primary nozzle test case.

Figure 2 shows the mesh resolutions for the primary nozzle case along the jet centerline and the lipline. Figures 3 and 4 compare the mean streamwise velocity and turbulent kinetic energy obtained from the four meshes. As the jet plume exits

the nozzle, turbulence intensifies along the shear layers, then grows in thickness as the jet expands further downstream. Sufficiently fine mesh grids are required in regions close to the jet lipline to resolve the energetically dominant turbulent scales. The nature of the Voronoi mesh introduces non-smooth grid resolution changes in the streamwise direction. As seen in the case with mesh A, such jumps in grid resolution truncate the continuous growth of turbulence along the shear layers and predict a shorter potential core length than observed with the other three meshes. This aspect is further indicated in Figure 5, which indicates that the lipline TKE profile contains spikes at locations where the grid coarsens in mesh A. From B to C, significant improvements in TKE are observed near the end of the jet potential core, between $x/D_e = 8$ and 10. From C to D, mesh grids between $x/D_e = 15$ and *20* are further refined but result in only minor improvement. Figure 6 shows the far-field acoustic predictions together with microphone measurements. Comparison of the results from mesh A, B, and C indicates that the grid improvement in the jet shear layers successively reduces the spurious hump at high frequencies. As expected, the results from mesh C and D show no significant variation. Even with the finest mesh, the LES results still differ from the measurements in two regions. For $St < 0.1$, LESs underpredict noise by as much as 3 dB at $\theta = 60^{\circ}$; for $St > 3$, the LES spectra have a faster falloff rate than indicated by the measurements. The exact reasons for these discrepancies are currently unknown.

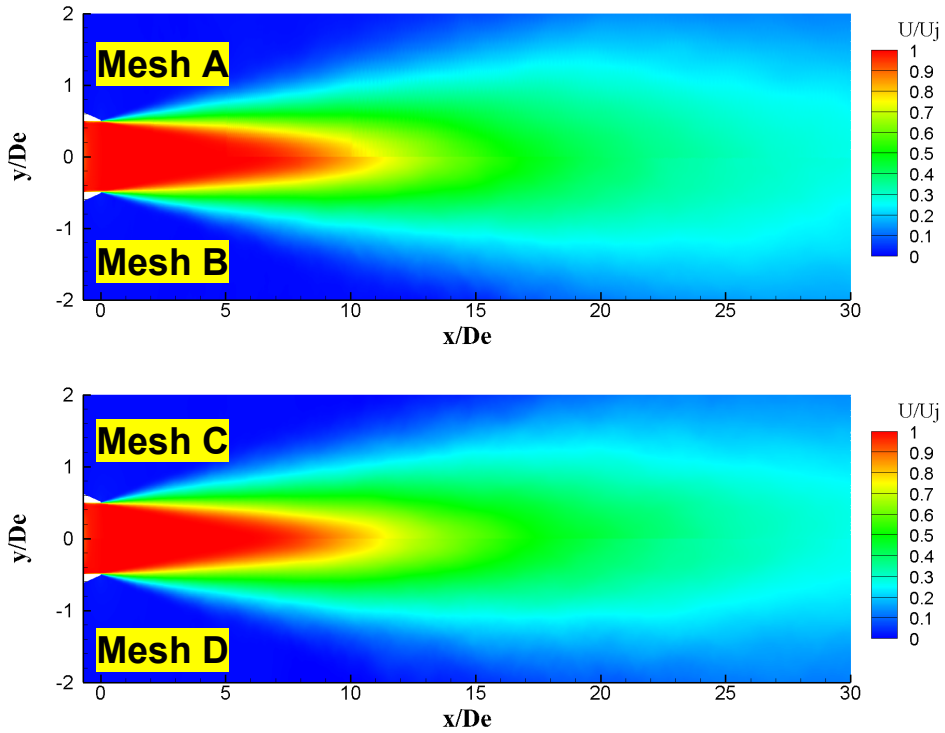

Figure 3. Comparison of mean streamwise velocity among all meshes for the primary nozzle case.

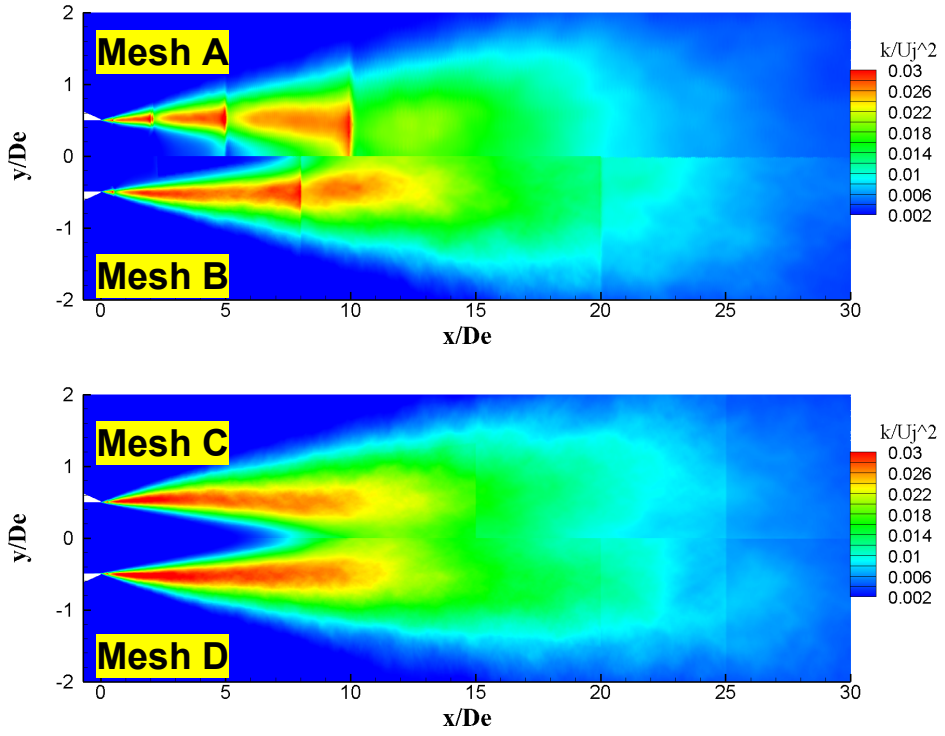

Figure 4. Comparison of mean turbulent kinetic energy among all meshes for the primary nozzle case.

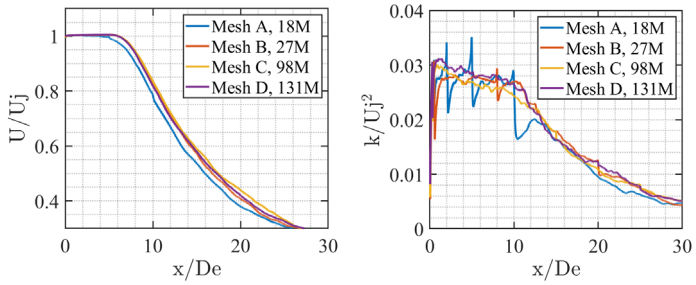

Figure 5. Comparison of mean centerline velocity (left) and lipline TKE (right) among all meshes for the primary nozzle case.

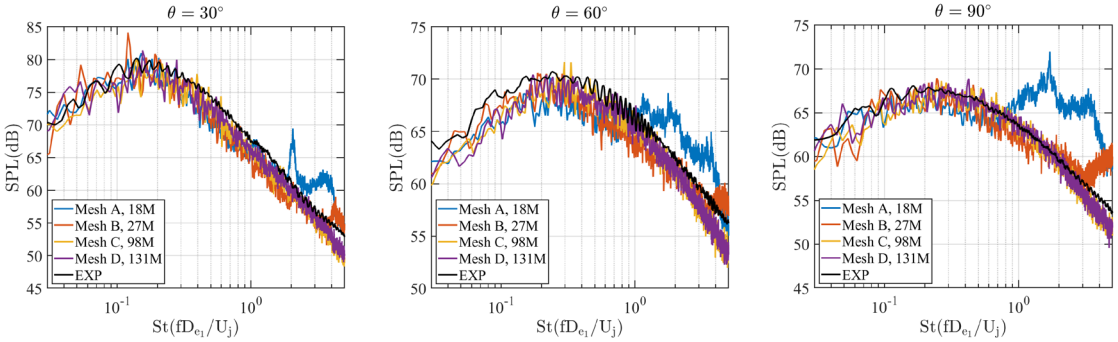

Figure 6. Comparison of acoustic spectra among all mesh cases and experiments.

On the basis of the lessons learned from the primary nozzle test case, the mesh for the co-annular nozzle test case is created such that the grids in the shear layers up to $x/D_e = 18$ are kept at $\Delta x/D_e = 0.025$, corresponding to a moderate mesh resolution similar to that of mesh B. Figures 7 and 8 compare the mean streamwise velocity between LES and PIV data. LES agrees with measurements well in terms of the overall jet spreading rate, potential core length, and the decay in the centerline jet velocity. Similarly to the primary nozzle case, the acoustic results from LES underpredict the noise at $St > 1$ (Figure 9), as expected because of the relatively modest but carefully tailored grid resolution. Near $St = 4$, the experimental data at $\theta = 30^{\circ}$ contain a small bump introduced by undesirable microphone vibrations (according to comments from the Georgia Tech team). This bump might further exacerbate the mismatch between LES and experimental results. The LES acoustic results can be further improved with a finer grid resolution, such as mesh C and D for the primary nozzle case.

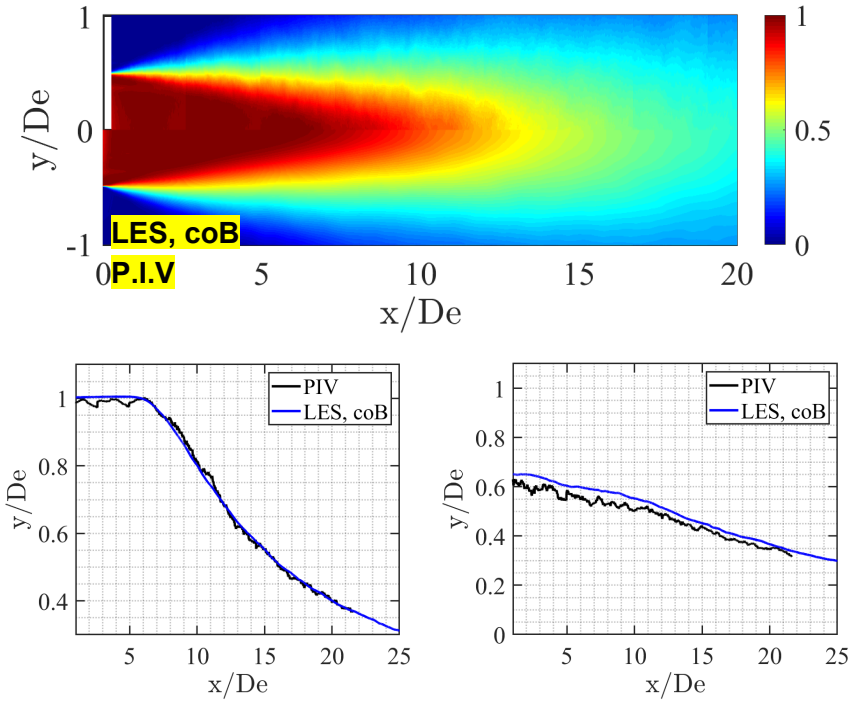

Figure 7. Comparison of mean streamwise velocity between experiments and LESs. Top: contour viewed in the midplane. Bottom left: centerline velocity profile. Bottom right: lipline velocity profile.

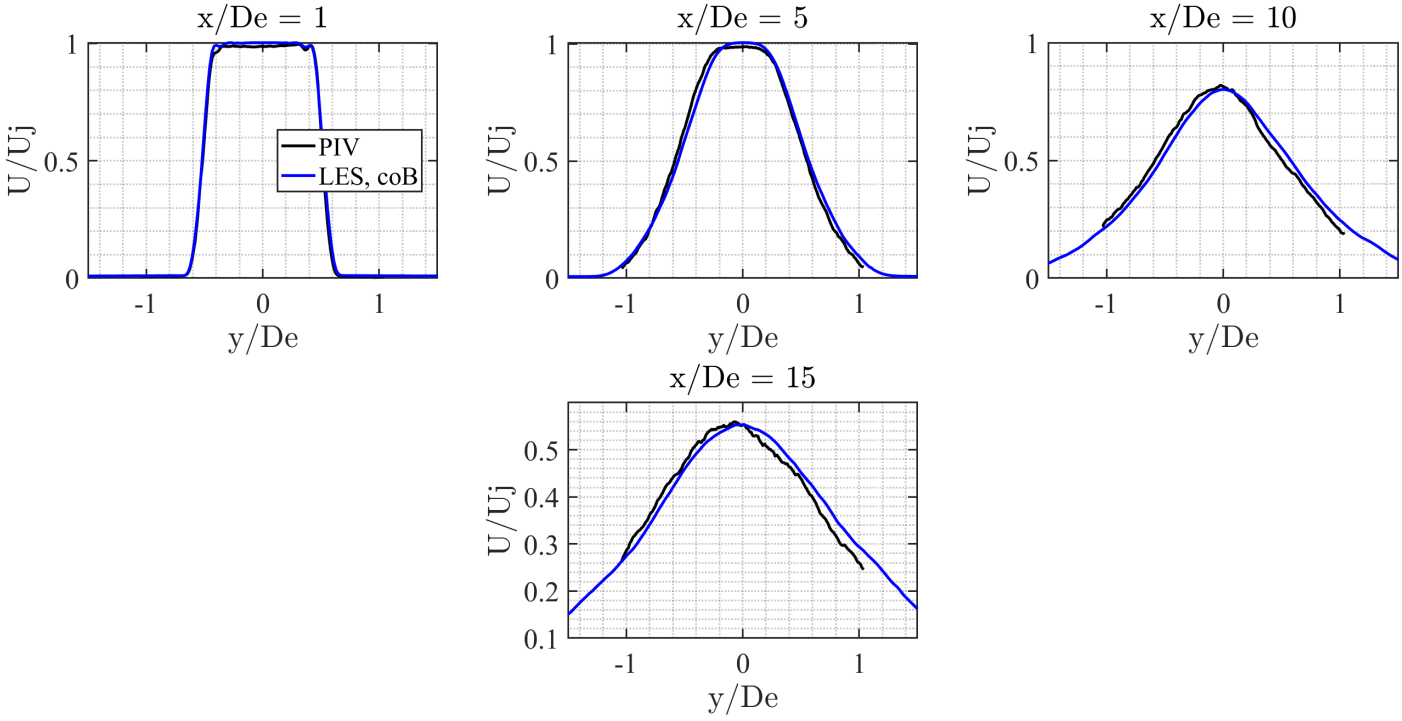

Figure 8. Radial profile comparison.

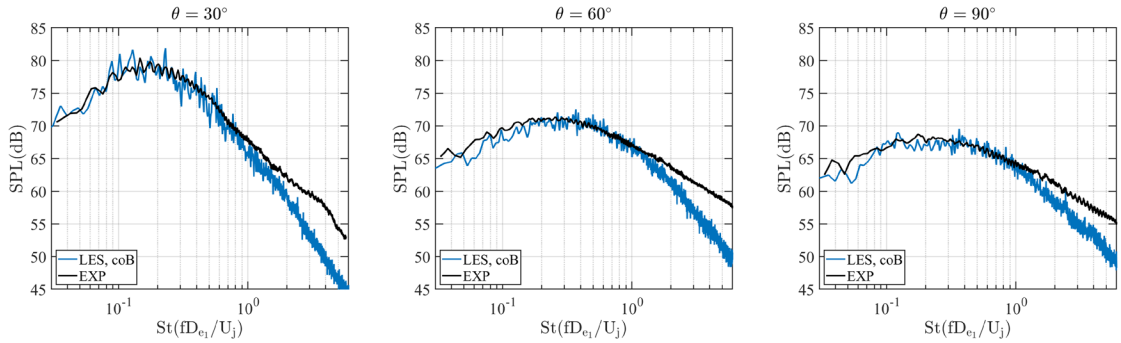

Figure 9. Comparison of acoustic spectra between LESs and experiments.

Milestones

LESs for test cases corresponding to the Georgia Tech. experimental test matrix have been significantly improved. Numerical errors due to insufficient grid resolution inside the jet shear layers have been identified and addressed.

Major Accomplishments

Over the past project year, we have made steady progress in high-fidelity simulations of jet noise, in accordance with the test plan set up by our Project 59 partners. LESs have been conducted for the Georgia Tech co-annular nozzle by using the compressible solver CharLES, developed by Cascade Technologies. The nozzle configuration with the shortest mixing duct, $L/D_e = 0.7$, is considered for two Mach numbers $M_j = 0.8$. The reason for the previously reported spurious high-frequency hump in the noise spectra has been identified through a detailed mesh sensitivity study. Because of insufficient resolution and aggressive coarsening of grids along the jet shear layers, the development of turbulent kinetic energy is inaccurately modeled, thereby resulting in the appearance of the high-frequency hump in the far-field SPL spectra. With improved grids,

the agreement between the LESs and experimental data for the mean velocity statistics is satisfactory, but discrepancies for far-field acoustics persist. Further investigation of the causes of such discrepancies is needed.

Publications

Published conference proceedings

Wu, G. J., Shanbhag, T. K., Molina, E. S., Lele, S. K., & Alonso, J. J. (2022, January 3). Numerical simulations and acoustic modeling of a co-annular nozzle with an internal mixing duct. *AIAA SCITECH 2022 Forum*. AIAA SCITECH 2022 Forum, San Diego, CA & Virtual. https://doi.org/10.2514/6.2022-2404

Outreach Efforts

Communication with Project 59 partners in ASCENT and with NASA scientists has been established. Deeper collaboration with the Georgia Tech experimenters and NASA scientists is expected as the project progresses further.

Awards

None.

Student Involvement

One graduate student, G. Wu, is involved in this project task.

Plans for Next Period

We plan to further refine the current LES results and achieve better agreement with experimental data. SPOD analysis with the LES data will be conducted to analyze the large-scale coherent structures associated with low-frequency acoustics. LES at additional flow conditions and geometries corresponding to the most recent experimental study at Georgia Tech and NASA Glenn Research Center will be performed.

Task 3 - RANS-based Simulation, Modeling and Validation of Jet Noise Predictions

Objectives

The project involves coordinated development of both low- and high-fidelity approaches for jet noise prediction. For the low-fidelity approach, RANS computations of a broader range of configurations and operating conditions relevant to civil supersonic aircraft will be performed and used to develop improved jet noise source models and more accurate far-field noise propagation kernels.

Research Approach

Ray tracing methods

In this work, we implement a RANS-based prediction method based on geometrical acoustics. Both the source model and the far-field propagation model use information obtained from a standard *k*-epsilon simulation of the jet flow. We perform all such simulations by using the open-source code SU2. The propagation model, which accounts for the effects of sound refraction, is based on a ray tracing method. This implementation makes very few simplifying assumptions regarding the flow field geometry and therefore is applicable to complicated nozzle configurations that result in inherently three-dimensional propagation effects. The highly parallel nature of the ray tracing algorithm also makes this method ideal for graphics-processing-unit implementation for accelerated analysis, optimization, and design. Our implementation of the source and propagation models as separate modules allows us to study their effects in isolation.

The presence of a moving medium and spatial gradients in the speed of sound significantly affect the refraction of sound waves reaching the far field. We account for these effects by introducing the flow factor, which represents the ratio of the pressure amplitude measured at the observer due to a particular source, with and without the jet flow being present. We make a high-frequency approximation to utilize the geometrical ray tracing method to describe wave propagation in non-uniform media. This method does not require the solution of an additional PDE over a domain extending to the far field, and it is well suited to complex and possibly asymmetric jet configurations. We follow Pierce's ray tracing formulation: a very large number of rays is launched from each acoustic source location, the path of each ray is computed by solving a governing

ODE for the velocity of a wavefront in a moving medium, and the pressure ratio along the ray tubes is subsequently computed by using the Blokhintsev invariant.

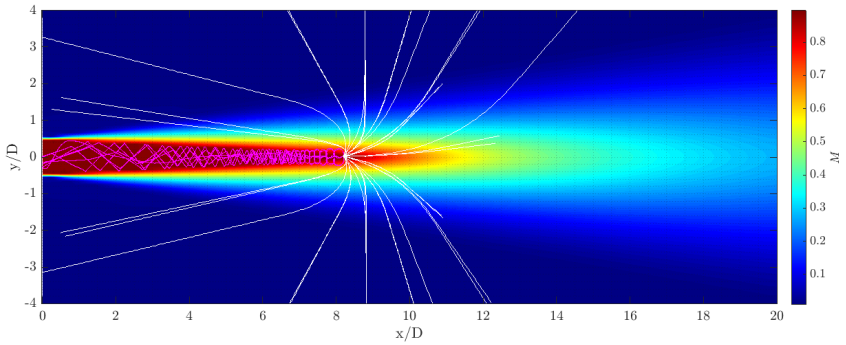

Figure 10. Ray path curvature due to flow refraction effects.

The effects of sound refraction by the jet flow can be observed in the paths taken by rays between the source locations and the far field. In the absence of any flow, and any flow gradients, each ray would follow a straight line from its source to its observer location on our chosen far-field sphere, following the angle at which it was launched. When the jet flow is included, a high degree of ray curvature exists in regions with high spatial gradients of velocity and sound speed. The flow factor is calculated by comparison of the number of rays that end at a given far-field location for the cases of no flow (straight rays) and jet flow (curved rays). Figure 10 shows the paths taken by a small number of rays being launched from an example source located close to the jet axis and to the end of the potential core. Some of the rays cross through the shear layer region, where velocity and speed-of-sound gradients along the ray paths are high. Consequently, these rays curve away from the jet axis. According to this observation, we expect that the addition of the flow factor will, in the case of acute polar observer angles, decrease the far-field SPL with respect to that obtained by using the source model alone. In contrast, in the case of obtuse polar angles, we expect to see the SPL increased by flow refraction effects. At an observer angle of 90°, the effects of refraction due to sound-flow interaction should be very small; therefore the flow factor is physically expected to be close to unity for all source locations. Notably, rays launched from this source location that fall within a critical range of launch angles remain trapped inside the jet's potential core. This behavior is physically expected: the rays undergo total internal reflection upon encountering a critically high value of local flow gradient transverse to the shear layer. The trapping of these rays and the corresponding reduction in effective acoustic propagation from inside this region to the far field leads to the conclusion that no significant concentration of true acoustic sources exists in the inviscid core. Therefore, in choosing the locations for the fictional sources in the ray tracing method, placing a very large number of sources inside this core is inefficient.

The effects of refraction on the computed far-field SPL may be studied in isolation by plotting the flow factor as a function of source location for different values of the polar observer angle. The flow factor is plotted in Figure 11 on a decibel scale for polar angles of 90° and 60° (with the azimuthal observer angle fixed at 90°) to demonstrate the net effect of ray curvature for sources in different regions of the jet plume. Positive values indicate refractive amplification, whereas negative values correspond to attenuation. For an observer located at 90°, the flow factor value is close to 1 everywhere, as expected; amplification due to refraction is negligible. However, at acute polar angles, in regions close to the nozzle exit where velocity and sound speed gradients are substantial, large shifts due to the effects of sound-flow interaction are observed. Much of the acoustic source region is attenuated, most significantly in the inviscid core, where total internal reflection is a dominating effect, as previously discussed. Moreover, the flow factor distribution is not axisymmetric, even for this axisymmetric round jet case. Sources located on the opposite side of the jet from the observer's location of interest are subjected to the greatest refraction shift. This finding is consistent with our observation of high ray curvature coincident with traversing of the shear layer. Sources located opposite from the observer must pass through these high-gradient regions twice before reaching the far field, thus resulting in a higher degree of ray scattering.

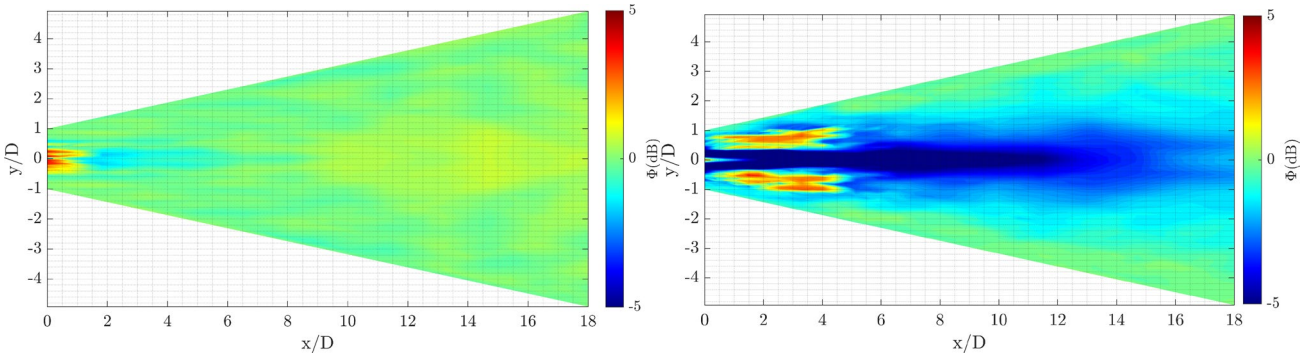

Figure 11. Flow factor for observer angles of (a) θ = 90° and (b) θ = 60°. The observer is above the plane of the figure (ϕ = 90°).

Optimization of turbulent time scales

For RANS methods to accurately model the turbulent correlation functions appearing in the source term of the Lighthill equation, a proper definition of the relevant turbulent length and time scales is required. Incorporating the inherent frequency dependence of these quantities has also been shown to be crucial for accurate acoustic prediction, particularly in the low- and high-frequency limits. Harper-Bourne (2000) originally proposed the form of the frequency dependence of length scales in low-Mach-number flows; this model was later applied by Morris and Boluriaan (2004), and implemented by Self (2004) in a statistical noise prediction framework. Self and Azarpeyvand (2009) further studied the frequency dependence of the length and time scales appearing in the source term definition of the MGBK method and proposed a new improved time scale accounting for the rate of transfer of turbulent energy between different wavenumbers.

In this work, we leverage information from LES of the jet flow emerging from a simple conical nozzle, to propose an improved form of the turbulent time scale for use in RANS-based jet noise prediction. From the unsteady LES data, the two-point velocity correlations are directly extracted for different locations in the flow field. We then apply several existing models for the characteristic turbulent scales from the literature. These models are used to compute predictions for the two-point correlation functions, which are compared with the true correlations extracted from the LES data. We derive the optimal spatially varying form of the turbulent time scale by optimizing a weight function over individual time scales that account for turbulent production, dissipation, and energy transfer within the jet. Studying the distribution of this weight function will allow us to determine which of these mechanisms dominate at different locations in the flow field. We hope that this approach will be generalizable to RANS-based acoustic prediction for other jet cases.

Figure 12 shows the fourth-order velocity fluctuation correlation computed at two different axial locations along the nozzle lipline for varying axial separations, and the corresponding Gaussian function approximations. Such function approximations have previously been used by authors to attempt to capture the effects of sound sources arising from both fine-scale turbulence and large-scale flow structures. Although the primary peak in the correlation may be well captured by a Gaussian fit, such a model form is unable to capture negative loops or secondary peaks, both of which are features associated with substantial flow inhomogeneity and are clearly present in this case. Therefore, in future work, a non-Gaussian fitting function that can capture these features may be advantageous; possible candidates include Bessel functions, exponential cosine mixtures, and Gaussian mixtures.

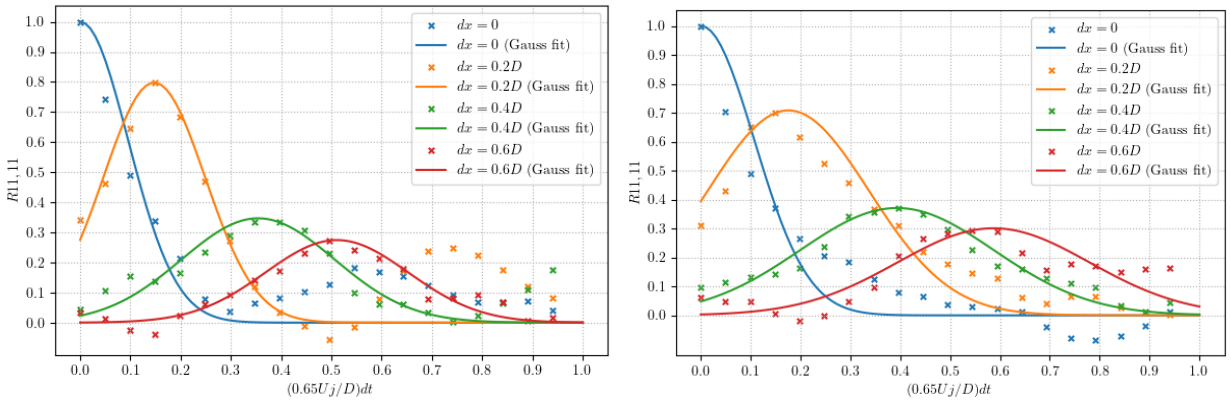

Figure 12. Gaussian fitting to the fourth-order two-point velocity correlation results, corresponding to the lipline $r/D = 0.5$ at (a) $x/D = 4$ and (b) $x/D = 6$.

In the same manner, we extract the fourth-order correlation at every point in the flow field and perform the same Gaussian fitting operation. This process allows us to obtain a spatially varying distribution of the characteristic time scale plotted in Figure 13a after averaging in the azimuthal direction and normalizing by the maximum field quantity (black dashed lines indicate the region occupied by the spreading turbulent jet). The velocity fluctuations over the potential core of the jet are correlated over quite small time scales and remain small along the jet centerline. Moving through the shear layer and the region where most acoustic sources are physically located, the time scale substantially varies; outside the spreading region of the flow, fluctuations appear to be correlated over a time period 4–5 times greater than that observed in the potential core. Figure 13b–d shows the characteristic time scales corresponding to turbulent dissipation, production, and energy transfer. By comparing these distributions against the findings in Figure 13a, we can more intuitively understand the different regions of the jet flow in which each mechanisms dominates and therefore is likely to be most influential when noise generation is computed.

In the region immediately downstream of the nozzle exit, the true distribution is best approximated by the production scale. Slightly further downstream, the dissipation and transfer scales become more relevant, capturing the contrast among short correlation scales along the core, larger scales outside of the spreading region, and a distinct pattern of short scales along the spreading region edges. Far downstream of the end of the potential core, the energy transfer scale appears to most closely resemble the true distribution, with large scales appearing relatively close to the axis. Figure 13e shows the normalized time scale distribution obtained by solving the weight optimization problem. This optimized field captures many qualitative features of the true distribution of time scales quite well.

Figure 14 shows the SPL computed by using the optimized scale distribution, compared with experimental results (experiments performed at Georgia Tech, narrow-bin SPL data obtained via private communication). The figure also shows the same spectrum computed by using the energy transfer scale proposed by Azarpeyvand and Self (2009); this scale is intended to reduce to that associated with different active turbulent mechanisms in regions of the flow where these dominate, and therefore should produce high-quality predictions across the band of relevant frequencies. The far-field spectrum computed with the optimized scales captures the overall spectrum shape very well across the full band of frequencies. A comparison of the optimized scale spectrum against the transfer scale spectrum indicates that both capture high-frequency falloff very well, and the optimized scale results in some improvement in low-frequency prediction; specifically, the flattening and overprediction observed in the transfer scale spectrum has been rectified. The transfer scale spectrum also slightly overpredicts the peak frequency of the spectrum; the optimized scale spectrum appears to do the opposite, underpredicting the peak frequency and slightly overpredicting the peak magnitude. For comparison, Figure 14 shows the same far-field SPL spectrum computed directly from LES data by using a permeable FW-H surface. The RANS-based acoustic predictions using the optimized time scale distribution produce a similar overall error compared with the experiment to FW-H. The FW-H computed spectrum better captures the overall spectrum shape but slightly underpredicts noise below $St = 0.2$, owing to insufficient simulation duration, and predicts a faster high-frequency falloff than that observed in the RANS or experimental result. The faster falloff for $St > 2$ probably results from a mismatch in jet initial shear layer turbulence from the experiment.

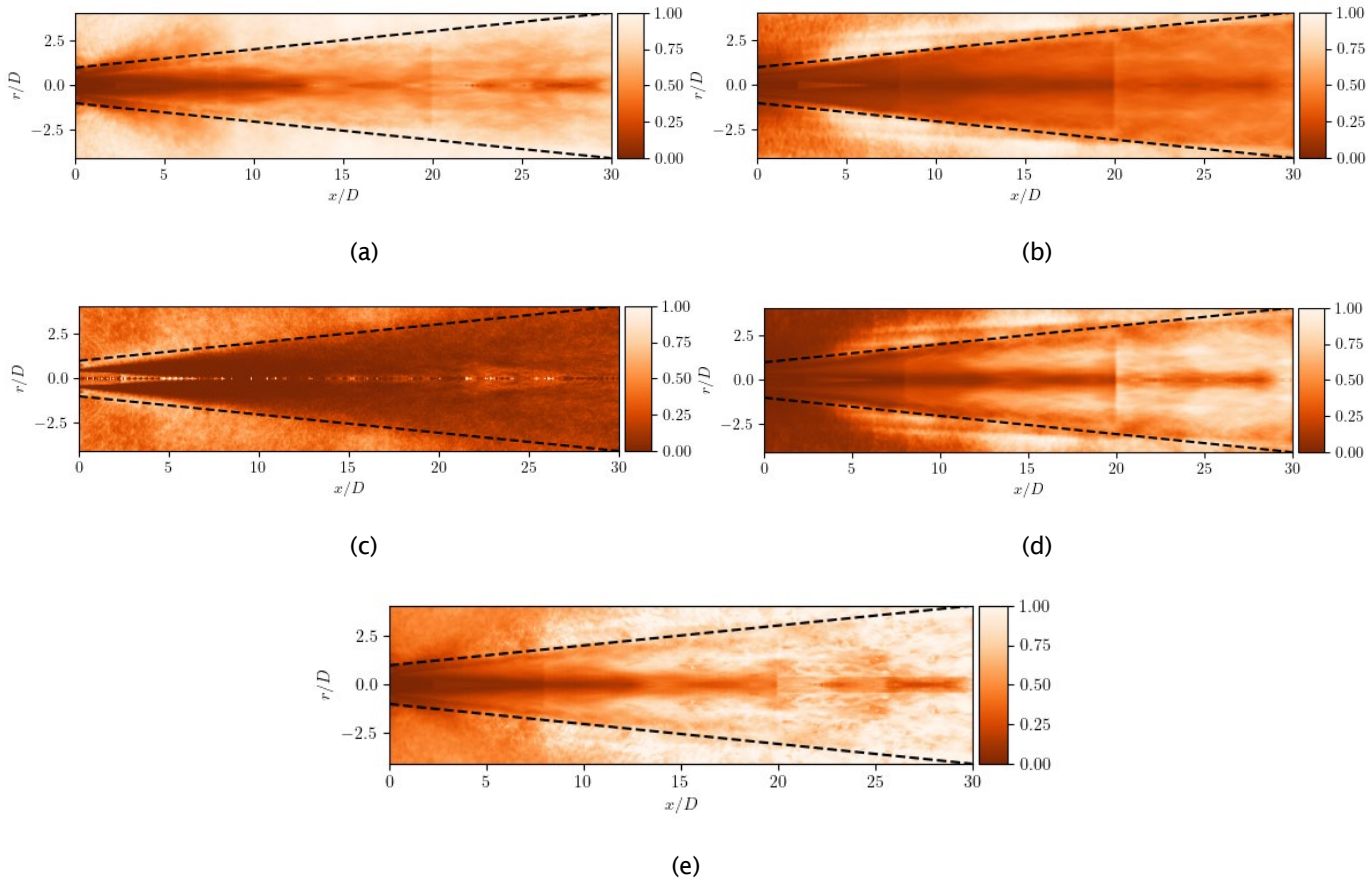

Figure 13. Spatial distribution of characteristic time scale: (a) true, computed from LES data, (b) dissipation, (c) production, (d) energy transfer and (e) optimized reconstruction.

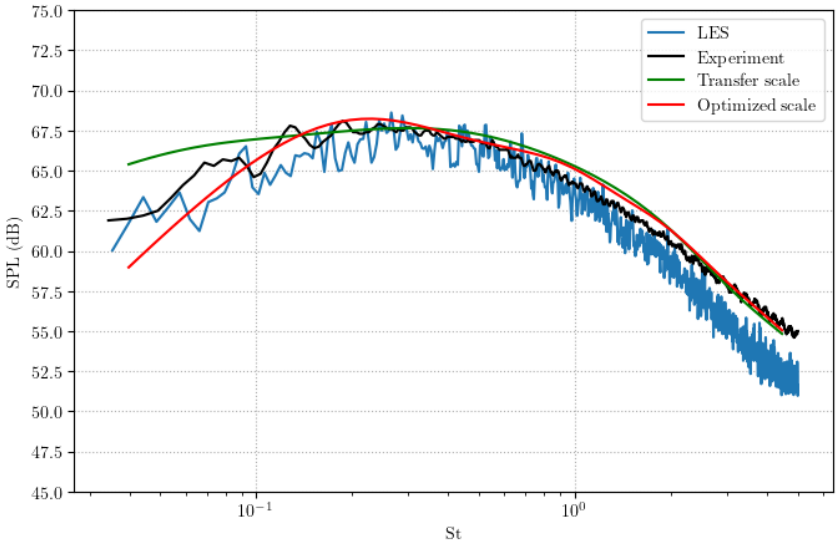

Figure 14. Far-field SPL at r = 75D, θ = 90°, computed by using LES-FW-H, energy transfer time scale, and optimized time scale, compared against experimental measurements.

Milestones

We have extended our modular implementation of the low-fidelity (RANS-based) acoustic prediction tool as described above, and tested it against experimental acoustic measurements for the Go4Hybrid round jet test case and the Georgia Tech primary nozzle test case.

Major Accomplishments

We have extended our previous source modeling implementation to include turbulent time scales based on different physical mechanisms. We have also proposed an optimization method to allow our source model to approximate the true turbulent correlations obtained from LES data. Our previous modular implementation of the low-fidelity acoustic model has been extended to include a far-field propagation tool based on the high-frequency geometrical method of ray tracing. This method is highly parallelizable and amenable to GPU implementation. We hope that this method will allow us to accelerate acoustic computation for the high-frequency part of the spectrum.

Publications

Published conference proceedings

Shanbhag, T. K., Zhou B. Y., Ilario, C. R. S., & Alonso, J. J. (2022, July). *Ray tracing methodology for jet noise prediction*. (ICCFD11-2022-1201). Eleventh International Conference on Computational Fluid Dynamics (ICCFD11).

Shanbhag, T. K., Wu, G. J., Lele, S. K., & Alonso, J. J. (2023, January 23). Optimization of turbulent time scales for jet noise prediction. *AIAA SCITECH 2023 Forum*. AIAA SCITECH 2023 Forum, National Harbor, MD & Online. https://doi.org/10.2514/6.2023-1159

Outreach Efforts

None.

Awards

None.

Student Involvement

T. Shanbhag has led the efforts with the ray tracing method for far-field propagation and optimization of time scales for improved acoustic source modeling described in the previous section.

Plans for Next Period

We will extend our work on optimized forms of the turbulent time scale in the acoustic source model, with an aim to propose a predictive form of this optimized scale that can be computed from RANS quantities alone. The source and propagation models have already been extended to automatic differentiation enabled implementations by using the Jax library. We hope to leverage this to begin to perform adjoint-based design optimization with far-field noise as an objective function to minimize.

References

Ahuja, K. K., Mavris, D. N., Tai, J., Karon, A. Z., Funk, R. B., and Ramsey, D. N. (2020. *Project 059B Jet Noise Modeling and Measurements to Support Reduced LTO Noise of Supersonic Aircraft Technology Development*. FAA ASCENT Annual Report.

Azarpeyvand, M., & Self, R. H. (2009). Improved jet noise modeling using a new time-scale. *The Journal of the Acoustical Society of America*, *126*(3), 1015–1025. https://doi.org/10.1121/1.3192221

Balsa, T. F., & Gliebe, P. R. (1977). Aerodynamics and noise of coaxial jets. *AIAA Journal*, *15*(11), 1550-1558.

Barber, T. J., Chiappetta, L. M., & Zysman, S. H. (1997). Assessment of jet noise analysis codes for multistream axisymmetric and forced mixer nozzles. *Journal of Propulsion and Power*, *13*(6), 737–744. https://doi.org/10.2514/2.5246

Blokhintzev, D. (1946). The propagation of sound in an inhomogeneous and moving medium i. *The Journal of the Acoustical Society of America*, *18*(2), 322–328. https://doi.org/10.1121/1.1916368

Brès, G. A., Ham, F. E., Nichols, J. W., & Lele, S. K. (2017). Unstructured large-eddy simulations of supersonic jets. *AIAA Journal*, *55*(4), 1164–1184. https://doi.org/10.2514/1.J055084

Brès, G. A., Bose, S. T., Emory, M., Ham, F. E., Schmidt, O. T., Rigas, G., & Colonius, T. (2018, June 25). Large-eddy simulations of co-annular turbulent jet using a Voronoi-based mesh generation framework. *2018 AIAA/CEAS Aeroacoustics Conference*. 2018 AIAA/CEAS Aeroacoustics Conference, Atlanta, Georgia. https://doi.org/10.2514/6.2018-3302

Bres, G. A., Towne, A., and Sanjiva, K. L. (2019). Investigating the effects of temperature non-uniformity on supersonic jet noise with large-eddy simulation. AIAA Paper 2019-2730.

Frendi, A., Nesman, T., & Wang, T.-S. (2002). On the effect of time scaling on the noise radiated by an engine plume. *Journal of Sound Vibration*, 256, 969–979.

Ilário, C. R. S., Azarpeyvand, M., Rosa, V., Self, R. H., & Meneghini, J. R. (2017). Prediction of jet mixing noise with Lighthill's Acoustic Analogy and geometrical acoustics. *The Journal of the Acoustical Society of America*, *141*(2), 1203–1213. https://doi.org/10.1121/1.4976076

Karon, A. Z. (2016). *Potential factors responsible for discrepancies in jet noise measurements of different studies* [Ph.D. thesis, Georgia Institute of Technology]. https://smartech.gatech.edu/handle/1853/56264?show=full

Khavaran, A., Krejsa, E., & Kim, C. (1992, January 6). Computation of supersonic jet mixing noise for an axisymmetric CD nozzle using k-epsilon turbulence model. *30th Aerospace Sciences Meeting and Exhibit*. 30th Aerospace Sciences Meeting and Exhibit, Reno,NV,U.S.A. https://doi.org/10.2514/6.1992-500

Harper-Bourne, M. (2000, June 12). Twin-jet near-field noise prediction. *6th Aeroacoustics Conference and Exhibit*. 6th Aeroacoustics Conference and Exhibit, Lahaina,HI,U.S.A. https://doi.org/10.2514/6.2000-2084

Karabasov, S. A., Afsar, M. Z., Hynes, T. P., Dowling, A. P., McMullan, W. A., Pokora, C. D., Page, G. J., & McGuirk, J. J. (2010). Jet noise: Acoustic analogy informed by large eddy simulation. *AIAA Journal*, *48*(7), 1312–1325. https://doi.org/10.2514/1.44689

Khavaran, A. (1999). Role of anisotropy in turbulent mixing noise. *AIAA Journal*, *37*(7), 832–841. https://doi.org/10.2514/2.7531

Khavaran, A., & Bridges, J. (2005). Modelling of fine-scale turbulence mixing noise. *Journal of Sound and Vibration*, *279*(3–5), 1131–1154. https://doi.org/10.1016/j.jsv.2003.11.054

Lighthill, M. J. (1952). On sound generated aerodynamically I. General theory. *Proceedings of the Royal Society of London. Series A. Mathematical and Physical Sciences*, *211*(1107), 564–587. https://doi.org/10.1098/rspa.1952.0060

Morris, P., & Boluriaan, S. (2004, May 10). The prediction of jet noise from cfd data. *10th AIAA/CEAS Aeroacoustics Conference*. 10th AIAA/CEAS Aeroacoustics Conference, Manchester, GREAT BRITAIN. https://doi.org/10.2514/6.2004-2977

Pierce, A. D. (1989). *Acoustics: An introduction to its physical principles and applications* (1989 ed). Acoustical Society of America.

Ribner, H. (1969). Quadrupole correlations governing the pattern of jet noise. *Journal of Fluid Mechanics, 38*(1), 1-24. doi:10.1017/S0022112069000012

Self, R. H. (2004). Jet noise prediction using the Lighthill acoustic analogy. *Journal of Sound and Vibration*, *275*(3–5), 757–768. https://doi.org/10.1016/j.jsv.2003.06.020

Tadmor, E. (2003). Entropy stability theory for difference approximations of nonlinear conservation laws and related time-dependent problems. *Acta Numerica, 12*, 451-512. doi:10.1017/S0962492902000156

Tam, C. K. W., & Auriault, L. (1999). Jet mixing noise from fine-scale turbulence. *AIAA Journal*, *37*(2), 145–153. https://doi.org/10.2514/2.691

Wundrow, D. W., & Khavaran, A. (2004). On the applicability of high-frequency approximations to Lilley's equation. *Journal of sound and vibration*, *272*(3-5), 793-830.